

Thermodynamics of Water Interaction with Human Stratum Corneum I: Measurement by Isothermal Calorimetry

SANTOSH YADAV,¹ NEVILLE G. PINTO,¹ GERALD B. KASTING²

¹Department of Chemical & Materials Engineering, University of Cincinnati, Cincinnati, Ohio 45221-0012

²College of Pharmacy, University of Cincinnati Medical Center, Cincinnati, Ohio 45267-0004

Received 16 May 2006; revised 28 July 2006; accepted 23 August 2006

Published online in Wiley InterScience (www.interscience.wiley.com). DOI 10.1002/jps.20781

ABSTRACT: A thermodynamic study of water interaction with human stratum corneum (SC) is presented. The procedure consisted of conjoint water vapor sorption and heat flow measurements. Heat of sorption of water in excised human SC at various relative humidities was measured in an isothermal calorimeter at 32°C using back and thigh skin from three different donors. These measurements, combined with the gravimetric sorption isotherm, were used to calculate the integral and differential enthalpies and entropies associated with binding of water to SC. Differential enthalpy values suggest hydrogen-bonding interactions similar to those for water in wool keratin. The changes in differential enthalpy and entropy with increasing water content followed a pattern similar to that seen in wool and other hydrophilic polymers. The results are partially interpreted in terms of a BET isotherm with monolayer volume $v_m = 0.022 \text{ g H}_2\text{O/g dry SC}$ and binding parameter $C = 6.5 \times 10^8$. © 2007 Wiley-Liss, Inc. and the American Pharmacists Association *J Pharm Sci* 96:1585–1597, 2007

Keywords: stratum corneum; water sorption; heat of sorption; calorimetry

INTRODUCTION

The stratum corneum (SC) acts as a protective layer between the highly hydrated viable epidermis and the relatively dry environment; thus it normally sustains a water activity gradient. The water content of SC is a function of relative humidity of the environment, SC barrier properties, and the presence of natural moisturizing factors (NMF). Skin hydration not only affects the barrier properties, but also affects the enzymatic activity in SC. This, in turn, affects the desquamation process and NMF level. The natural hydration level of SC *in vivo* is around 30%–

40% of its dry weight. It has been observed that when SC is equilibrated in saturated water vapor¹ or in pure liquid water,² its mass increases to 300%–400% of its dry weight. Water acts as a natural penetration enhancer, increasing the flux of hydrophilic as well as lipophilic substances. It has been reported that penetration of water increased by a factor of two- to three fold in fully hydrated versus partially hydrated skin.¹ This study and many others (see Reference 3 and references therein) suggest that when the amount of water exceeds 20%–30% by weight of the SC dry weight, the excess water may be characterized as free water, having the same properties as bulk water. Bouwstra et al.¹ focused on water distribution in human SC and swelling of the corneocytes. They showed that water at a hydration level of 300% w/w (3 g H₂O/g dry SC) slightly changes the lipid transition in SC compared to dry SC, and

Correspondence to: Gerald B. Kasting (Telephone: 513-558-1817; Fax: 513-558-1978; E-mail: Gerald.Kasting@uc.edu)

Journal of Pharmaceutical Sciences, Vol. 96, 1585–1597 (2007)
© 2007 Wiley-Liss, Inc. and the American Pharmacists Association

that water is nonuniformly distributed in the SC. It is mainly present within the corneocytes and not in the intercellular regions. They also observed a linear relationship between corneocyte thickness and hydration level of the SC.

Calorimetry has long been used to study the interactions of liquids and gases with solid substrates.^{4–10} Much early and often very high quality work employed adiabatic methods, exemplified by Morrison's studies of water sorption in wool and other natural fibers.^{4–6} Isothermal methods have been used to study water and carbon dioxide absorption on natural and synthetic polymers.^{7–9} An excellent article by O'Neill et al.¹⁰ outlines the capabilities of these systems. For SC, however, most calorimetric studies have been conducted using temperature scanning methods. Differential scanning calorimetric (DSC) and differential thermal analysis (DTA) studies have been conducted using SC equilibrated at different water contents, providing information about lipid and protein structural changes at different temperatures.^{11–23} Some of the studies as well as equilibrium water binding²⁴ have been conducted on isolated powders comprised of plantar SC samples in which the ultra-structural changes between the intercellular components of SC may not be well reproduced.^{12,23} In addition, there is still a lack of thermodynamic information associated with structural modification. The microscopic changes in SC may be advantageously described in terms of thermodynamic properties. Leveque et al.²⁵ made strides in this area using isothermal calorimetry, but provided only a limited analysis of these data. El-Shimi and Princen²⁶ studied sorption and desorption of water vapor from human, pig, and rat SC using gravimetric analysis. They observed hysteresis in the sorption–desorption isotherms. Water content during desorption was higher than that during sorption for the range of 10%–50% relative humidity, possibly due to strain in the protein matrix during desorption. Furthermore, they calculated the isosteric heat of sorption of water uptake in female SC to be -94.3 kJ/mol using sorption data at two different temperatures, 32 and 36°C, by applying the Clausius–Clapeyron equation,

$$\Delta H_{\text{iso}} = \frac{RT_1 T_2}{(T_1 - T_2)} \ln \frac{p_1}{p_2} \quad (1)$$

In Eq. 1, p_1 and p_2 are partial pressures at equal uptake of water vapor at temperatures T_1 and T_2 , respectively, and ΔH_{iso} is the isosteric heat of sorption. Negative values of ΔH_{iso} imply an

exothermic reaction. El-Shimi and Princen²⁶ observed that the magnitude of ΔH_{iso} decreased as the water content increased; at approximately 15% water uptake its absolute value was just higher than that of the latent heat of vaporization, H_L . The Clausius–Clapeyron equation is derived for an ideal equilibrium system which exhibits no hysteresis between adsorption and desorption; results derived from it are furthermore quite sensitive to errors in the sorption data. SC is comprised of lipid and proteins which do show a hysteresis for water sorption,²⁶ and accurate sorption measurements at low RH are difficult.³ Therefore, conclusions based on these results may not reflect the actual energetics of sorption of water in SC. Spencer et al.²⁷ performed a similar set of studies with the opposite result, that is, ΔH_{iso} was found to be positive (endothermic reaction) although the magnitude still decreased with increasing water content. The limitations of these results draw our attention to calorimetry, which can produce direct information about the heat of sorption.

In this article, isothermal microcalorimetry was used to study the interaction between water vapor and isolated human SC. The objective was to provide a better understanding of water balance in skin, a key factor in maintenance of healthy skin condition.

MATERIALS AND METHODS

Chemicals

All chemicals were reagent grade. Trypsin, trypsin inhibitor Type II from soybean and Nile red were purchased from Sigma Chemical Company (St. Louis, MO). Phosphate-buffered saline (pH 7.4, 10 mM) was prepared from anhydrous NaH_2PO_4 (1.9 mM), anhydrous Na_2HPO_4 (8.1 mM), and NaCl (150 mM), all from Fisher Scientific (Pittsburgh, PA). Compressed dry air was provided by Wright Brothers, Inc. (Cincinnati, OH). Distilled water was used for all studies.

Human Skin

Cryoprotected, cadaveric, split-thickness human skin from thigh and back (stored in 10% glycerol) was obtained from US Tissue and Cell (Cincinnati, OH) and stored at -80°C until use. Donors were 50–70 years of age. Epidermis was obtained from dermis by heat separation at 60°C for

2 min.²⁸ Isolated SC was prepared by trypsinization of epidermis (0.01% trypsin overnight) followed by trypsin inhibitor. It has been reported that SC sheets so prepared possess considerable chemical and mechanical resistance and have permeabilities similar to unprocessed skin specimens.²⁸ The sample mass varied from 10 to 15 mg. Isolated SC was dried over silica gel in a N₂ atmosphere at room temperature for 24 h. The SC samples were further dehydrated by placing them above P₂O₅ in a closed vessel at 30°C. Bright field and fluorescence microscopy examination of these samples confirmed they were comprised of anuclear, cornified cells as expected for SC. Two days before the calorimetric studies, dried and weighed SC sheets were hydrated in distilled water for 30 min, and then placed on stainless steel inserts. Special precaution was taken during sample preparation to avoid overlapping the tissue upon itself, so that the SC sheets spread uniformly on the stainless steel insert. The prepared SC samples were dried and dehydrated in a vacuum desiccator for 72 h at 25°C, then stored in a desiccator at 4°C until use.

Calorimeter System

All heat flow studies were performed using a Setaram C80D microcalorimeter (Astra Scientific, Inc., Danville, CA). This instrument has a sensitivity of approximately 10 μW. The C80 calorimeter has a sample and a reference vessel, each possessing a volume of 12.5 mL, into which various types of the cells may be inserted. Two types of cells were used in this study: standard cells for calibration with indium and gallium, and

gas circulation cells for heat flow measurements with SC.⁸ The calibration was conducted by melting the metals in the temperature scanning mode, and the SC studies were conducted by sorbing water vapor into the tissue in the isothermal mode at 32°C. The calorimeter measures the difference in the heat flow between sample and reference cells.

Gas flow was controlled by mass flow controllers (Microscal, London, UK) and calibrated by bubble flow meters (SGE, Austin, TX). A hygrometer/thermometer/dew point meter (Control Company, Friendswood, TX) was used to measure humidity. Relative humidity was adjusted by metering dry and humid air in an appropriate ratio. Two humidifiers in series were used to obtain the desired humidity level. The humidifier temperature was maintained at 32°C by a heater. All SC samples and the calorimeter were evacuated at room temperature for a minimum of 48 h using a mechanical pump. Heat flow signals were displayed in real time via a printer. A schematic of the experimental setup is shown in Figure 1.

Software

Thermal Analysis Software provided by Instrument Specialist (Spring Grove, IL) was used for all studies. The software had two sections: DSC data acquisition software (version 4.0.376) was used to measure and record the emf representing the heat flow, and TAS pro software (version 4.2.14) was used to integrate the signals. A data acquisition system (Control Company, version 2.22) was used to record the humidity throughout the experiments.

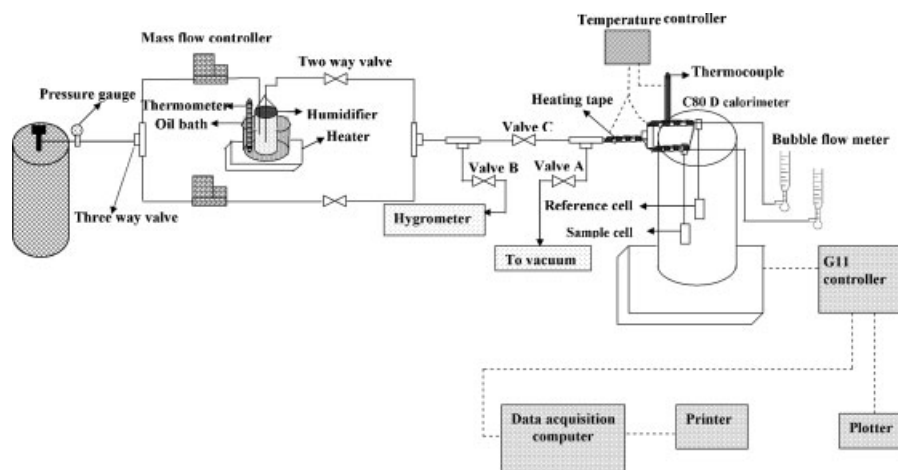


Figure 1. Experimental setup for heat of sorption studies.

Temperature Control

Humidified air was supplied to the calorimeter using stainless steel tubing. The temperature of the inlet air stream was controlled by a temperature controller (Model-Barant, Port Huron, MI) using a type K thermocouple sensor. Tubing earlier in the air stream was wrapped with insulating tape to minimize temperature variation throughout the apparatus.

Calibration

The heat flow calibration for the C-80 instrument was initially set at the factory using Joule heating cells with the calorimeter operated in the isothermal mode. The calibration was checked in our laboratory via a scanning measurement of the heat of fusion of gallium and indium metals in standard vessels. The temperature of the calorimeter was varied from 25 to 200°C for indium and from 25 to 40°C for gallium. The heat of fusion was calculated by Thermal Analysis Software, without modification to the factory heat flow calibration. The results obtained for melting temperature and enthalpy of fusion were within 2% of literature values.²⁹ Each metal was studied at least three times at three different scanning rates. Results obtained at different scanning rates were in good agreement.

Heat of Sorption Measurements

Heat flow measurements for water vapor sorption on SC were conducted in gas circulation vessels. The cells had input and output ports. The inlets of both cells were connected to the humidified air stream fed at a controlled and measured relative humidity. The weighed and dried SC sample on stainless steel insert was placed in the sample cell, and an identical stainless steel insert without SC was placed in the reference cell. By opening Valve A (Fig. 1), both cells were subjected to vacuum for 24 h to remove water and any other volatile components from the sample. The outputs valves of both vessels were closed during evacuation. The relative humidity in the vapor generator was adjusted to the desired level by opening Valve B. When steady state was attained, water vapor at a calibrated relative humidity and measured temperature was fed to the microcalorimeter cells by opening Valve C and closing Valves A and B. Although all significant (i.e., above baseline) heat evolution occurred within the first several hours, the gas was allowed

to flow for 24 h to ensure equilibrium. The outlet ports of both cells were connected to identical bubble soap meters to measure the actual flow rates. Periodically, the experiment was conducted without any sample present to test for artifacts and baseline drift. There was no difference between the heat flow signal and the baseline values with no gas flowing.

Data Analysis

The water vapor sorption isotherm together with calorimetric measurements can be used to calculate the thermodynamic properties of water-polymer systems. This combination of methods has been developed by various investigators and applied to a number of hydrophilic polymers including silk fibroin,⁴ wool keratin,⁵ fibrous cellulose,⁶ and microcrystalline cellulose.⁷

We have calculated the thermodynamic properties for water vapor sorption on human SC with respect to relative humidity and moles of adsorbate. The analysis derives from Hollenbeck et al.'s⁷ analysis of heat of immersion of microcrystalline cellulose. A schematic of water vapor sorption by vapor phase and immersion is shown in Figure 2. The net enthalpy change associated with vapor phase adsorption is the difference between heat of immersion (Step 1) and heat of vaporization (Step 2). Thus we follow Hollenbeck's⁷ analysis, but consider also the effect of the condensation of water vapor to a liquid.

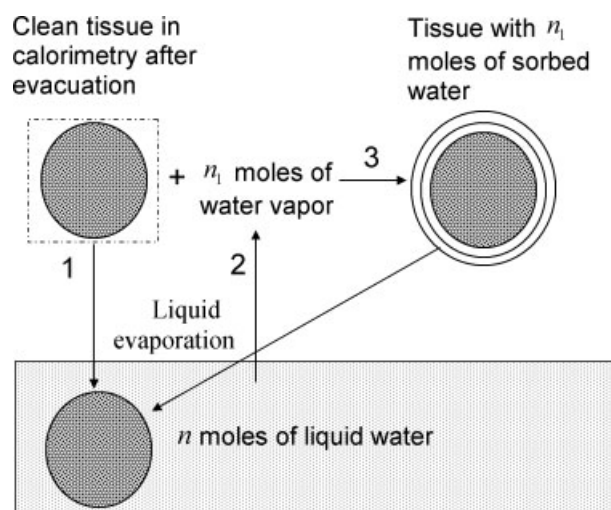


Figure 2. Schematic of thermodynamic model for water vapor adsorption on solid (adapted from Hollenbeck et al.⁷).

Free Energy Changes

Let Component 1 be a volatile liquid and Component 2 be a nonvolatile solid. At constant temperature, the net integral free energy change ΔF for sorption of n_1 moles of liquid onto n_2 moles of solid is⁷

$$\Delta F = \overline{\Delta F}_1 n_1 + \overline{\Delta F}_2 n_2 \quad (2)$$

In Eq. 2 $\overline{\Delta F}_1$ and $\overline{\Delta F}_2$ are the partial molal free energy changes of the volatile and nonvolatile components, respectively. The partial molal properties are considered as differential properties with respect to number of moles of water sorbed. The integral and differential free energy changes can be obtained from the equilibrium sorption isotherm.⁷ The total differential of Eq. 2 is

$$d\Delta F = \overline{\Delta F}_1 \cdot dn_1 + n_1 \cdot d\overline{\Delta F}_1 + \overline{\Delta F}_2 \cdot dn_2 + n_2 \cdot d\overline{\Delta F}_2 \quad (3)$$

According to the Gibbs–Duhem relationship,

$$n_1 \cdot d\overline{\Delta F}_1 + n_2 \cdot d\overline{\Delta F}_2 = 0 \quad (4)$$

The differential free energy change for a liquid adsorbate, $\overline{\Delta F}_1$, is the difference between the chemical potential of the liquid adsorbate μ_1 and that of pure liquid μ_1^0 ;⁷ thus

$$\overline{\Delta F}_1 = \mu_1 - \mu_1^0 = RT \ln \frac{p}{p_0} \quad (5)$$

Here p/p_0 is relative vapor pressure at the experimental temperature T , and R is the universal gas constant.

Integrating Eq. 4 and substituting the value of $\overline{\Delta F}_1$ from Eq. 5,

$$\overline{\Delta F}_2 = -RT \int \left(\frac{n_1}{n_2} \right) d \left(\ln \frac{p}{p_0} \right) \quad (6)$$

Substituting the value of $\overline{\Delta F}_2$ from Eq. 6 into Eq. 2,

$$\Delta F = n_1 RT \ln \frac{p}{p_0} - RT \int_0^{p/p_0} n_1 d \ln \frac{p}{p_0} \quad (7)$$

$$\Delta F = n_1 RT \ln \frac{p}{p_0} - RT \int_0^{p/p_0} n_1 \frac{p_0}{p_1} d \left(\frac{p}{p_0} \right) \quad (8)$$

The water sorption isotherms were used to calculate the differential $\overline{\Delta F}_1$ and integral ΔF free

energy changes associated with water sorption using Eqs. 5 and 8, respectively. The evaluation of the integral on the right hand side of Eq. 8 can be performed graphically from the plot of $n_1 p_0/p$ versus p/p_0 . Using this approach the error associated with low pressure extrapolation to $p=0$ is smaller than the plot of n_1 versus $\ln(p/p_0)$.⁷ The unit of $\overline{\Delta F}_1$ is kJ per mole of the adsorbate and that of ΔF , as written, kilojoules. For comparison with the other keratinized tissues, we will choose n_1 and n_2 such that ΔF applies to 100 g of dry SC plus associated water. For simplicity, $\overline{\Delta F}_1$ and n_1 are replaced by $\overline{\Delta F}$ and n in the remainder of the text.

Enthalpy Changes

The integral enthalpy change (ΔH) of water sorption can be determined directly from calorimetric signals at various relative humidities. To calculate ΔH from these measurements, a linear baseline was established at each relative pressure by connecting the baseline before and after the pressure change in the system. The area between the heat flow curves and baseline was determined by Thermal Analysis Software. As a test, the enthalpy changes were recorded with no SC sample in the calorimeter; the reference and sample cells contained only the inserts. The enthalpy change was zero. The unit of integral enthalpy change ΔH is kilojoule per 100 g of dry adsorbent.

The differential or partial molal enthalpy change of the system associated with water vapor sorption ($\overline{\Delta H}_1$), was obtained by numerically differentiating ΔH with respect to number of moles of water sorbed using a two-point method, then plotting each result at the midpoint; thus

$$\overline{\Delta H}_1 = \left(\frac{\partial(\Delta H)}{\partial n_1} \right)_{n_2, P, T} \approx \frac{\Delta(\Delta H)}{\Delta n_1} \quad (9)$$

The differential enthalpy change of water binding $\overline{\Delta H}$ can be defined as the difference between $\overline{\Delta H}_1$ and the excess latent heat H_L associated with water condensation at temperature T :

$$\overline{\Delta H} = \overline{\Delta H}_1 - H_L \quad (10)$$

where $H_L = -43.64$ kJ/mol at 32°C.⁵ The units of $\overline{\Delta H}$, $\overline{\Delta H}_1$, and H_L are kilojoule per mole of water. $\overline{\Delta H}$ reflects the net enthalpy produced from swelling (endothermic) and water vapor sorption (exothermic). The average value of $\overline{\Delta H}$ was calculated by first: making a plot of $\overline{\Delta H}$ versus n

(mol H₂O/100 g dry SC) and then making a graphical interpolation of the $\overline{\Delta H}$ value at equally spaced points (every 0.05 mol H₂O/100 g dry SC) for the samples included in the average.

Entropy Changes

Once the differential and integral enthalpies and free energies are determined, both the integral and differential entropy changes can be determined by subtraction. The integral entropy change is

$$\Delta S = \frac{(\Delta H - \Delta F)}{T} \quad (11)$$

and the differential entropy change is

$$\overline{\Delta S} = \frac{(\overline{\Delta H} - \overline{\Delta F})}{T} \quad (12)$$

The units of ΔS are J/K/100 g dry SC and of $\overline{\Delta S}$ are J/K/mole of water.

BET Water Sorption Model

The Brunauer, Emmet, and Teller (BET) isotherm considers short-range interactions between adsorbate and adsorbent.³⁰ Adsorbed molecules beyond the first layer on the adsorbent are assumed to be bulk liquid. This two parameter model yields a Type II or Type III sorption isotherm in IUPAC nomenclature. The BET isotherm can be expressed as follows:

$$\frac{v}{v_m} = \frac{Cx}{(1-x)(1-x+Cx)} \quad (13)$$

where v is the equilibrium water content, v_m is the monolayer water content, $x = p/p_0$ is the equilibrium water activity (or relative pressure), and C is a binding parameter that can be expressed as $C = c_0 \exp[(H_1 - H_L)/RT]$ where c_0 is a ratio of partition functions in the first and subsequent layers, H_1 is molar enthalpy of adsorption in the first layer [kJ/mol], and H_L is molar enthalpy for condensation of bulk liquid [kJ/mol]. A purely enthalpic interpretation of C yields $c_0 = 1$.³¹ This choice, as will be shown, leads to extremely high values for C . We will adopt this interpretation for the present report and relax this restriction as well as consider other isotherm models in a separate analysis. In this article we are concerned only with the value of the monolayer volume v_m , which is relatively insensitive to c_0 .

The BET model parameters C and v_m were fitted to experimental values of water sorption and

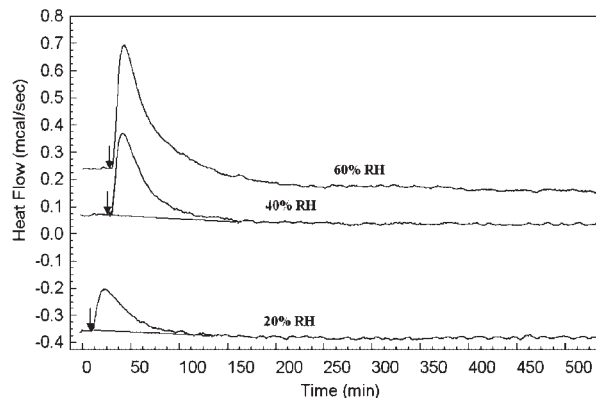


Figure 3. Representative heat flow profiles for water sorption onto human SC at 32°C. The data plotted here were obtained on a sample of thigh skin from Donor-3 Thigh. For clarity, the profiles were offset from 0 by -0.035 mcal/s (20% RH), 0.08 mcal/s (40% RH), and 0.25 mcal/s (60% RH). Arrows indicate the starting of the water vapor sorption on tissue.

sorption enthalpies for all samples by a least squares nonlinear regression analysis that will be described elsewhere. The basis of the sorption enthalpy calculation is described by Pudipeddi et al.⁹

RESULTS

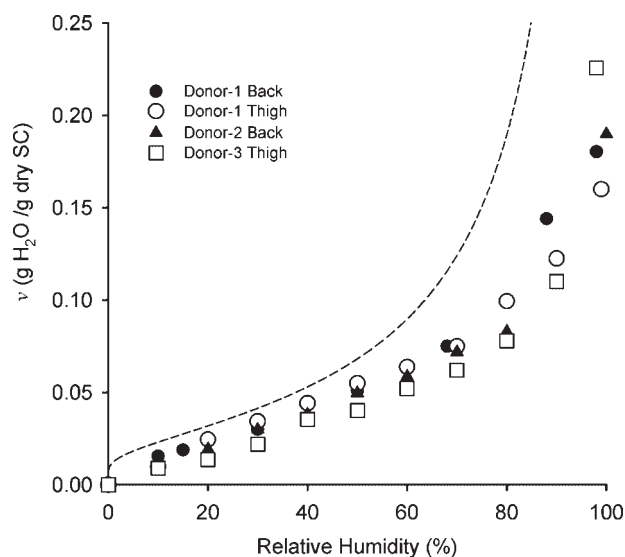


Figure 4. Water content of SC samples obtained after heat flow measurements at 32°C. Each symbol represents the mean of two samples. The dashed curve represents the average water sorption values from six laboratories reported in Kasting and Barai.³

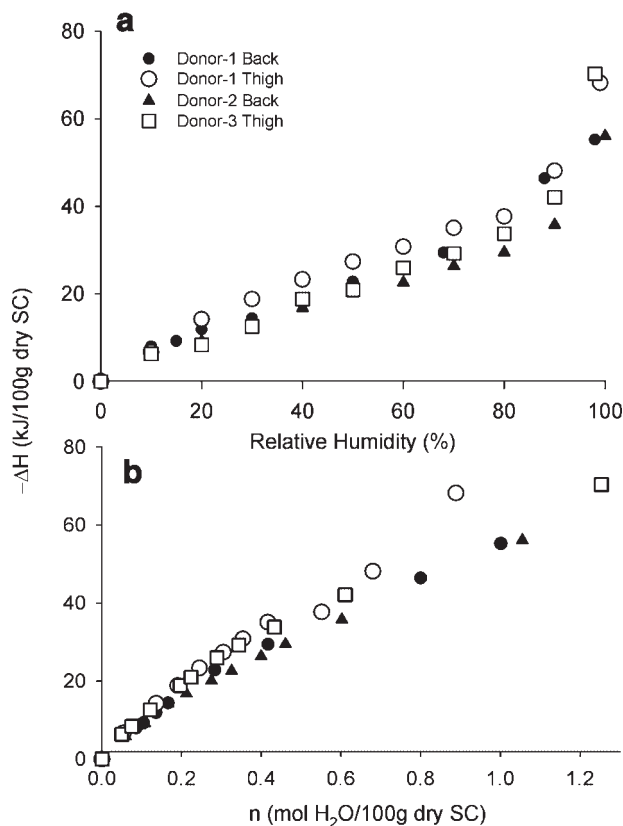


Figure 5. Integral enthalpy from heat flow measurement plotted (a) versus relative humidity (b) versus moles of water per grams of dry SC. Enthalpy values were calculated as shown in Figure 3.

Figure 3 shows representative heat flow profiles associated with water vapor sorption onto human SC in the isothermal calorimetry system. Most of the heat evolution as analyzed occurred within the first 2 h. The average amounts of water sorbed in the calorimeter at the completion of each 12–15 h exposure measured gravimetrically, are shown in Figure 4 as a function of the relative humidity of the inlet air stream. The integral enthalpies calculated from the heat flow measurements are shown in Figure 5, plotted first versus relative humidity (Fig. 5a) and then versus the amounts of water sorbed (Fig. 5b). These data were subjected to a thermodynamic analysis as described in the Materials and Methods. The analysis involved both a model-independent approach (Eqs. 2–12) and a comparison with specific isotherm models, for example, the BET model (Eq. 13). Model-independent results and a brief summary of the BET analysis are reported here. Full details of the isotherm analysis will be given elsewhere.

Integration of the data in Figure 4 according to Eq. 8 yielded the integral free energy change of the

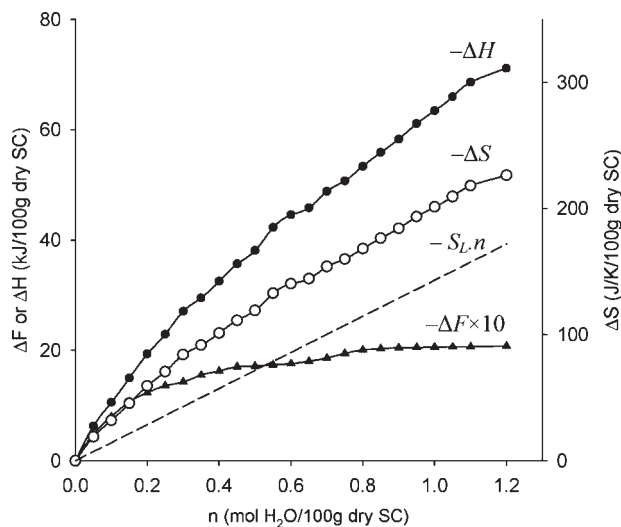


Figure 6. The integral thermodynamic properties for water sorption on human SC. These values were calculated as interpolated averages of three donors (Donor-1 Back, Donor-2 Back, Donor-3 Thigh). The integral free energy values have been multiplied by 10 for clarity. The dashed line represents the contribution of the entropy of condensation to $-\Delta S$.

system for water vapor sorption onto SC, ΔF . The combination of these values with ΔH (Fig. 5a) according to Eq. 11 yielded ΔS . The average change in the integral thermodynamic properties for three of the four pairs of samples as a function of moles of water sorbed are plotted in Figure 6. The samples identified as Donor-1 thigh were considered separately for the reasons discussed below. Numerical differentiation of the data in Figure 5b according to Eq. 9 followed by subtraction of the latent heat of condensation (Eq. 10) yielded the partial molar enthalpies of water binding $\overline{\Delta H}$ shown in Figure 7. Inspection of these results showed that three of the pairs of skin samples showed similar long-range interactions with water (middle region of graph), whereas the Donor-1 thigh samples had a substantially higher binding enthalpy in this region. This difference led us to analyze these samples separately. A smooth curve was drawn through the three like sets of data by linearly interpolating between data points and then averaging the interpolated values. This procedure led to the solid line in Figure 7. A smooth curve representing the Donor-1 thigh samples (dashed line) was hand drawn for comparison. At low water content, the value of $-\overline{\Delta H}$ (mean \pm SD) was 62 ± 17 kJ/mol for the three like donors and 82 kJ/mol for the Donor-1 thigh samples. For all samples, the magnitude of $-\overline{\Delta H}$

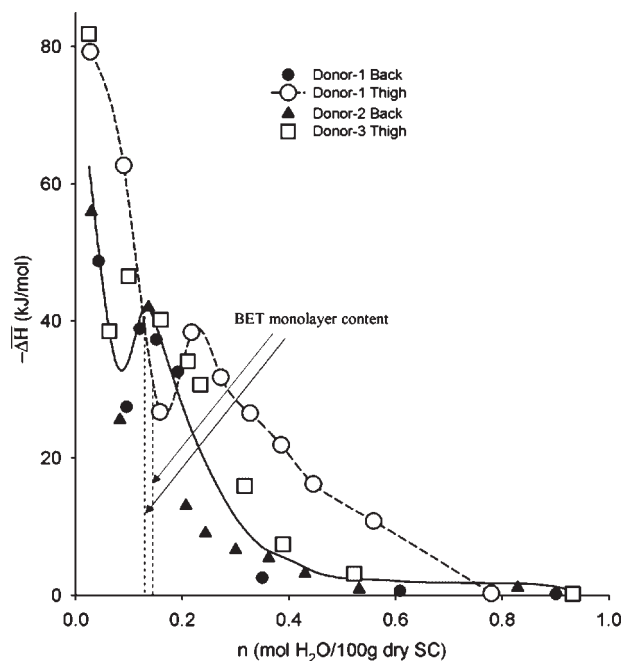


Figure 7. Differential enthalpy of water binding plotted as a function number of moles of water adsorbed. The solid line is the interpolated average of three donors (Donor-1 Back, Donor-2 Back, and Donor-3 Thigh) and the dashed line represents Donor-1 Thigh.

decreased rapidly with increasing water content up to $n = 0.1$ mol $\text{H}_2\text{O}/100$ g dry SC, reflecting less exothermic interactions with the tissue. Above this value of n , there was a small but sharp maximum in $-\overline{\Delta H}$ that was seen in all the samples tested, as well as the averages plotted in Figure 7. The peak occurred at slightly higher water content for the Donor-1 thigh samples. These features occurred at a water content either equal to or slightly above the monolayer value arising from a BET analysis of these data (cf. Eq. 13). For water contents above $n = 0.2$ mol $\text{H}_2\text{O}/100$ g all samples showed a rapid decline in $-\overline{\Delta H}$, leading to values not significantly different from zero for n greater than 0.6–0.8 mol $\text{H}_2\text{O}/100$ g dry SC, depending on the sample. In this region, the enthalpy of water sorption in the SC was indistinguishable from the condensation of water vapor to bulk water. This does not imply that all water sorbed above this value behaves in the tissue as free water, as discussed later.

Differential free energy $\overline{\Delta F}$ and entropy $\overline{\Delta S}$ values associated with water sorption in SC were constructed for the three like pairs of samples using Eqs. 5 and 12, respectively. The curve for $\overline{\Delta S}$ was calculated using the average $\overline{\Delta H}$ values in Figure 7. Results are shown in Figure 8. Because the latent heat of condensation H_L was subtracted

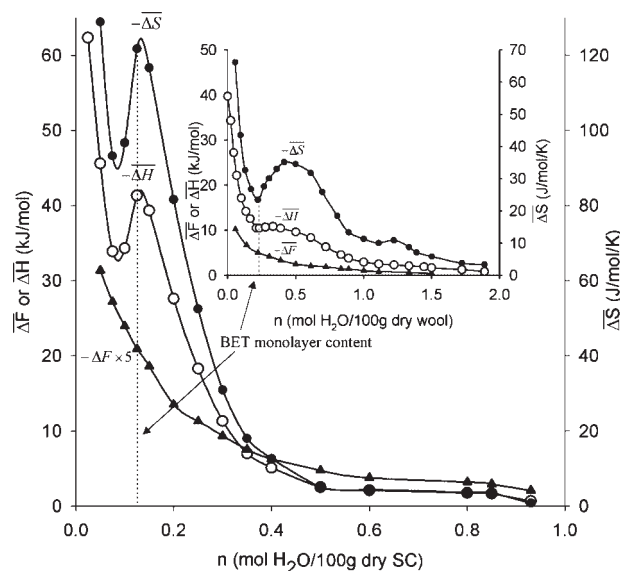


Figure 8. Average differential thermodynamic properties of three donors. These values were calculated as interpolated averages of Donor-1 Back, Donor-2 Back, and Donor-3 Thigh samples. The differential free energy values have been multiplied by a factor of 5 of clarity. Inset shows the differential thermodynamic properties of water vapor sorption on wool (Morrison and Hanlan⁵).

from $\overline{\Delta H}_1$ in order to calculate $\overline{\Delta H}$ (Eq. 10), values of $\overline{\Delta S}$ so calculated reflect entropy changes beyond that associated with the condensation of water vapor to a liquid ($S_L = H_L/T = -143.0$ J/mol/K at 32°C). Thus, negative values of $\overline{\Delta S}$ (corresponding to positive values of $-\overline{\Delta S}$ in the figure) reflect an increase in order with incremental addition of water, beyond that of water condensation which would add another -143.0 J/mol/K to the value of $\overline{\Delta S}$ for the system. The negative values of $\overline{\Delta S}$ in Figure 8 primarily reflect the binding of water into a low mobility state, as discussed later.

DISCUSSION

The interaction of water with the SC has been the subject of study for more than 50 years. Important tools for measuring these effects *ex vivo* include mechanical testing,^{24,32} sorption isotherms,^{3,24,26} X-ray diffraction,³³ neutron diffraction,³⁴ NMR spectroscopy,^{35–37} IR spectroscopy,³⁵ DSC,^{11–15,18–23} and DTA.^{16,17} Limited isothermal calorimetry results have been reported.²⁵ The calorimetric study reported here represents, to our knowledge, the first detailed energetic analysis of SC/water

interactions. These results complement information obtained by other techniques and allow for a direct comparison with the energetics of water interaction with wool,⁵ silk protein,⁵ and cellulosic polymers.^{6,7}

Most investigators agree that a substantial amount of the water present in SC in its normal, air-dried state is bound to the tissue to various degrees, giving it properties that differ from bulk water. Exact proportions vary according to the technique, but the nonfreezable water content of 0.34 g H₂O/g dry SC in human limb obtained by DSC,¹³ corresponding to $n = 1.9$ mol H₂O/100 g dry SC, is representative. It has frequently been noted that this value is considerably higher than the water content that can reasonably be associated with a single bound monolayer surrounding the keratin fibers;^{3,13,26,35,38} thus, there is evidence for long range interactions with the tissue. The picture is complicated by the fact that keratin fibers uncoil as they hydrate, exposing more primary binding sites.^{32,39} Furthermore, the intercellular lipids in SC bind a small amount of water in the head group region,^{11,37} and low molecular weight solutes or NMF within the corneocytes contribute a heat of dilution as the corneocyte swells. The present study integrates all of these effects. The results suggest that the energetics of water interaction with the SC is dominated by keratin, as shown by comparison with the water-wool system (Inset to Fig. 8).

According to the chosen analysis (Fig. 3) heat evolution associated with water vapor sorption onto SC occurred predominately in the first 2 h following exposure and was essentially complete after 4 h. The measurements do not preclude a gradual release of heat extending over a much longer period; in fact, such a release is possible as SC continues to swell for days following exposure to high humidities^{3,40} or liquid water.^{1,41} However, the amounts of water found in the tissue at the conclusion of each exposure were smaller than those found in more extended studies of SC water sorption, especially at high values of RH (Fig. 4 and References 1 and 2). This finding suggests that the extended swelling associated with liquid phase immersion did not occur. Swelling of a polymer network is an endothermic phenomenon involving rupturing of the solid-solid bonds.⁷ For solids in which swelling is predominant, the heat of wetting is lower because some of the released heat is consumed in swelling. It is furthermore possible that the SC samples did not experience the full RH measured external to the calorimeter due to temperature variations within the system or to

calibration error. Such an error would not impact the shape or magnitude of the differential thermodynamic properties shown in Figures 7 and 8, which are accurate over the range of water content shown (0–1 mol H₂O/100 g dry SC). Additional water sorption at high RH could lead to an extended “tail” of the differential properties similar to that seen for wool (inset to Fig. 8). However, the properties of the additional water would be close enough to bulk values (cf. Fig. 7 in which $-\overline{\Delta H}$ approaches zero at high values of n) that it is unlikely that it could be distinguished from bulk water by the present technique.

The cadaver skin evaluated in this study was cryopreserved with glycerol (a humectant), frozen, thawed, trypsinized, and later heat-separated. Each of these steps may have an impact on the results. We note that these procedures are commonly employed in skin permeation work, with the result that acceptable barrier properties are usually maintained. The glycerol used for storage was partially washed from the tissue during the rinsing and trypsinization procedures. The fact that water sorption was low compared to literature values rather than high (Fig. 4) suggests that the results are not strongly impacted by residual glycerol. To test this hypothesis we conducted a heat of solution experiment at 32°C with 0.5 mL of glycerol and 2.0 mL of water. The result was $\Delta H_{\text{soln}} = -12.0$ J/g of glycerol (exothermic). If the SC in our studies had retained as much as 5% glycerol after processing (a reasonable upper limit), then heat evolution from this tissue upon hydration could have contained a glycerol-related ΔH_{soln} component of about 60 J/100 g dry SC. Comparison of this value with the total enthalpy change in the system of about 60 kJ/100 g dry SC (Fig. 5b) shows that ΔH_{soln} of glycerol would contribute only 0.1% of the total integrated signal. However, a complete answer to the question of glycerol storage and other tissue processing steps awaits a study of freshly excised human skin combined with an alternative technique for preparing SC.

The monotonic increases in integral values of $-\Delta F$, $-\Delta H$, and $-\Delta S$ with increasing RH (Fig. 6) confirm that SC water sorption is a spontaneous, enthalpically driven process over the full range of water content tested. Negative values of ΔS (corresponding to positive values of $-\Delta S$) indicate that the system taken as a whole becomes more ordered as the sorption process progresses. A large component of this ordering is the entropy of condensation, $S_{\text{L}} = -143.0$ J/mol/K at 32°C, shown

as a dashed line in Figure 6. The calculated ΔS values are more negative than would be calculated for bulk water condensation, reflecting the additional ordering due to localization of the bound water molecules. This effect is offset by the disordering of the keratin fibers in the SC component of the system. The balance is clearly shown by the differential properties plot in Figure 8, where the value of S_L has been subtracted prior to calculating $\overline{\Delta S}$.

The differential plots shown in Figures 7 and 8 provide a particularly sensitive measure of water interactions with SC. These plots show how the thermodynamic properties of the system vary for infinitesimal changes in water content (cf. Eq. 9). These differential properties show a qualitative similarity to the thermodynamic properties of the water/wool system⁵ (inset to Fig. 8). The latter were generated by a combination of water vapor sorption (to obtain $\overline{\Delta F}$) and heat of immersion of partially hydrated wool (to obtain $\overline{\Delta H}$). For both wool and SC, the initial sorption of water within the dry tissue was strongly exothermic, with enthalpies ranging from -40.0 kJ/mol for wool to $-(67 \pm 17)$ kJ/mol for SC (Fig. 7). This water was highly immobilized, since $\overline{\Delta S}$ was large and negative (Fig. 8). It may be considered to be chemisorbed. As more water was taken in, $-\overline{\Delta H}$ and $-\overline{\Delta S}$ fell rapidly, reflecting weaker interactions with the tissue and greater mobility. For wool, there was a plateau in the enthalpy values at $-\overline{\Delta H} \cong 11$ kJ/mol and water contents of 0.2–0.4 mol/100 g dry SC which Morrison attributed to monolayer completion in the BET sense.⁵ For SC there was an inflection point in the enthalpy for all of the samples at water contents of 0.1–0.2 mol/100 g dry SC, yielding a minimum and a maximum within this region; however, the peak enthalpy values were in the range 38–48 kJ/mol, approximately four times the plateau value for wool. It is not clear that these features are comparable in the two tissues, but it may be noted that both are in the range of the estimated monolayer coverage accord-

ing to a BET analysis [0.39 mol H₂O/100 g dry tissue for wool and 0.12 mol H₂O/g dry tissue for SC (Tab. 1)]. Morrison considered the rapid decrease in $-\overline{\Delta H}$ prior to the plateau to be associated with the energy required to disrupt or “peptize” the dried keratin gel, since $-\overline{\Delta S}$ fell rapidly in the same range of water content. Based on the results in Figure 8, a similar argument may be made for SC at water contents well below the BET monolayer value. However, as the monolayer is completed, swelling evidently slows in the SC, leading to larger observed values of $-\overline{\Delta H}$ and $-\overline{\Delta S}$. This follows since swelling is an endothermic and disordering process. It should be noted that $-\overline{\Delta S}$ in the SC falls with increasing water content from a value initially twice that of wool. Thus, the data support that the initial water sorbed by SC is more tightly bound and consequently less mobile than that in wool. It seems possible that binding of water to the head groups in SC intercellular lipids may account for these differences. A calorimetric study of delipidized SC to investigate this possibility is underway.

The Donor-1 thigh samples had longer range interactions with water than did the other three pairs of samples, based on the data in Figure 7. These samples had values of ($-\overline{\Delta H} \cong 16$ kJ/mol at $n = 0.4$ – 0.5 mol H₂O/100 g dry SC, higher than the values for wool in this range of water content. At higher values of n , the situation was reversed. The value of $-\overline{\Delta H}$ fell to zero (within experimental error) at $n = 0.8$ mol H₂O/100 g dry SC. For the other samples the drop in $-\overline{\Delta H}$ was even more rapid. Recall that water sorbed in this range of hydration is still considered bound when examined by NMR or DSC techniques.^{13,35} These data suggest that the “binding” observed for water in the range $n = 0.5$ – 1.9 mol H₂O/100 g dry SC (corresponding to $v = 0.09$ – 0.34 g H₂O/g dry SC or an SC water content of 8–25% w/w) results from a weak enthalpic interaction resulting in the partial immobilization of several layers of water around keratin fibers. According to an estimate

Table 1. BET Model Parameters Obtained from Nonlinear Regression Analysis

Donor	Site	$C \times 10^8$	v_m , g H ₂ O/g Dry SC	H_1 , kJ/mol
Donor-1	Back	6.82	0.020	95.27
	Thigh	5.16	0.025	94.56
Donor-2	Back	6.67	0.022	95.19
Donor-3	Thigh	7.18	0.022	95.31
	Mean \pm SD	6.46 \pm 0.89	0.022 \pm 0.002 ^a	95.08 \pm 0.35

^aThis value corresponds to $n = 0.12 \pm 0.01$ mol H₂O/100 g dry SC.

derived from water mobility arguments, the immobilized layer is approximately 5 Å or 2.3 water molecules thick.³⁸ This thickness corresponds to a bound water volume of $v = 0.30$ g H₂O/g dry SC or $n = 1.7$ mol H₂O/100 g dry SC. Considering that our samples were very small and we are determining $-\overline{\Delta H}$ by subtracting a substantial latent heat from $-\overline{\Delta H}_1$ (Eq. 10), it is probable that we cannot accurately measure the small enthalpy differences from bulk water corresponding to the more loosely bound water in the tissue.

While differences between water interactions with wool and SC are evident, much larger differences are found between these two tissues and other hydrophilic polymer systems. For the water-silk fibroin system the maximum values of $-\overline{\Delta H}$ and $-\overline{\Delta S}$ were 20 kJ/mol and 22 J/mol/K, respectively.⁴ Comparable values were found for water in cotton cellulose.⁶ Microcrystalline cellulose yielded a flatter profile for $-\overline{\Delta H}$ in the water content range below $n = 0.15$ mol H₂O/100 g of solid with a plateau value of 15 kJ/mol.⁷ The investigators attributed the plateau to the combination of no swelling with an energetically homogeneous surface. None of the natural fibers or tissues studied showed a comparable feature at low water content.

There has been one previous calorimetric study of water sorption in SC conducted by a similar method. Leveque et al.²⁵ studied water sorption at 19°C on intact, delipidized, and delipidized/water-washed samples of human abdominal SC. The calorimetric equivalent of $-\overline{\Delta H}$ was reported in kJ/mol, although the heat of condensation ($H_L = -44.22$ kJ/mol at 19°C) was not subtracted from the result. After making this subtraction, Leveque's²⁵ average values for intact SC have a maximum $-\overline{\Delta H}$ value of 14 kJ/mol in dry SC and fall to zero at a water content of $v = 0.13$ g H₂O/g dry SC or $n = 0.7$ mol H₂O/100 g dry SC. For higher water contents they fall in the endothermic range, that is, the reported heat evolution was less than the latent heat, resulting in a positive value of $\overline{\Delta H}$. The magnitude of these results is not consistent with our measurements or those for the other water-polymer systems discussed above. The study does suggest that the major contributors to $\overline{\Delta H}$ in SC are keratin and NMF, since the order of enthalpies (expressed as $-\overline{\Delta H}$) was: intact SC \sim delipidized SC $>$ delipidized/water-washed SC. A follow-up study to confirm this result and improve upon the absolute values is in progress.

SUMMARY

The enthalpy and entropy of water sorption in SC are consistent with a picture in which water first binds tightly to polar sites on keratin, replacing keratin-keratin bonds with energetically favorable keratin-water bonds. This process swells and softens the tissue, leading to rapid decreases in the magnitudes of the differential thermodynamic properties $\overline{\Delta H}$ and $\overline{\Delta S}$ with increasing water content. The calculated values of these properties are reminiscent of those associated with water binding in wool keratin and silk fibroin, but have higher magnitudes at low water content. At water contents above 0.14 g H₂O/g dry tissue (0.8 mol/100 g dry SC), the enthalpy of water vapor sorption was indistinguishable from the heat of condensation of liquid water, yet water sorbed in this region (up to 0.34 g H₂O/g dry tissue) is found to be bound when studied by other techniques. This loosely associated water is thus intermediate in nature between a strongly bound monolayer and bulk water.

NOMENCLATURE

C	$c_0 \exp[(H_1 - H_L)/RT]$, BET binding parameter [dimensionless]
H_1	Molar enthalpy of adsorption in the first layer [kJ/mol]
H_L	Molar enthalpy of condensation of bulk liquid [kJ/mol]
ΔH_{iso}	Isosteric heat of sorption [kJ/mol]
$\overline{\Delta H}$	Differential enthalpy change of water binding [kJ/mol]
$\overline{\Delta S}$	Differential entropy change of water binding [J/mol/K]
$\overline{\Delta F}$	Differential free energy change [kJ/mol]
$\overline{\Delta H}_1$	Differential enthalpy change [kJ/mol]
ΔH	Integral enthalpy change [kJ/100 g dry SC]
ΔS	Integral entropy change [J/K/100 g dry SC]
ΔF	Integral free energy change [kJ/100 g dry SC]
n	Moles of water adsorbed [mol H ₂ O/100 g dry SC]
R	Universal gas constant [J/mol/K]
T	Temperature [K]
v	Equilibrium water content [g H ₂ O/g dry SC]
v_m	Monolayer water content [g H ₂ O/g dry SC]
x	Relative vapor pressure of the gas [p/p ₀]

ACKNOWLEDGMENTS

We wish to acknowledge a fellowship (SY) from A. William Forbriger and partial support from NIOSH/CDC grant R01 OH07529.

REFERENCES

- Bouwstra JA, de Graaff A, Gooris GS, Nijssse J, Wiechers JW, van Aelst AC. 2003. Water distribution and related morphology in human stratum corneum at different hydration levels. *J Invest Dermatol* 120:750–758.
- Warner RR, Stone KJ, Boissy YL. 2003. Hydration disrupts human stratum corneum ultra-structure. *J Invest Dermatol* 120:275–284.
- Kasting GB, Barai ND. 2003. Equilibrium water sorption in human stratum corneum. *J Pharm Sci* 92:1624–1631.
- Dunford HB, Morrison JL. 1955. The heat of wetting of silk fibroin by water. *Can J Chem* 33:904–912.
- Morrison JL, Hanlan JF. 1957. Swelling of fibrous proteins. *Nature* 179:528.
- Morrison JL, Dzieciuch MA. 1959. The thermodynamic properties of the system cellulose-water vapor. *Can J Chem* 37:1379–1390.
- Hollenbeck RG, Peck GE, Kildsig DO. 1978. Application of immersional calorimetry to investigation of solid-liquid interactions: Microcrystalline cellulose-water system. *J Pharm Sci* 67:1599–1606.
- Banerjee T, Chhajer M, Lipscomb GG. 1995. Direct measurements of the heat of carbon dioxide sorption in polymeric materials. *Macromolecules* 28:8563–8570.
- Pudipeddi M, Sokolowski TD, Duddu SP, Carstensen JT. 1996. Quantitative characterization of adsorption isotherms using isothermal microcalorimetry. *J Pharm Sci* 85:381–386.
- O'Neill MAA, Gaisford S, Beezer AE, Skaria CV, Sears P. 2006. A comparison of the performance of calorimeters application of a test and reference reaction. *J Therm Anal Cal* 84:301–306.
- Imokawa G, Kuno H, Kawai M. 1991. Stratum corneum lipids serve as a bound-water modulator. *J Invest Dermatol* 96:845–851.
- Inoue T, Tsujii K, Okamoto K, Toda K. 1986. Differential scanning calorimetric studies on the melting behavior of water in stratum corneum. *J Invest Dermatol* 86:689–693.
- Walkley K. 1972. Bound water in stratum corneum measured by differential scanning calorimetry. *J Invest Dermatol* 59:225–227.
- Wickett RR. 1987. A review of stratum corneum plasticization mechanisms. *Bioeng Skin* 3:383–388.
- Potts RO, Golden GM, Francoeur ML, Mak Vivien HW, Guy RH. 1991. Mechanism and enhancement of solute transport across the stratum corneum. *J Control Release* 15:249–260.
- Wilkes GL, Nguyen AL, Wildenauer RH. 1973. Structure-property relations of human and neonatal rat stratum corneum. I. Thermal stability of the crystalline lipid structure as studied by X-ray diffraction and differential thermal analysis. *Biochim Biophys Acta* 304:267–275.
- Bouwstra JA, de Vries MA, Gooris GS, Bras W, Brussee J, Ponc M. 1991. Thermodynamic and structural aspects of the skin barrier. *J Control Release* 15:209–220.
- Rehfeld SJ, Elias PM. 1982. Mammalian stratum corneum contains physiologic lipid thermal transitions. *J Invest Dermatol* 79:1–3.
- Van Duzee BF. 1975. Thermal analysis of human stratum corneum. *J Invest Dermatol* 65:404–408.
- Golden GM, Guzek DB, Harris RR, McKie JE, Potts RO. 1986. Lipid thermotropic transitions in human stratum corneum. *J Invest Dermatol* 86:255–259.
- Tanojo H, Bouwstra JA, Junginger HE, Bodde HE. 1999. Thermal analysis studies on human skin and skin barrier modulation by fatty acids and propylene glycol. *J Therm Anal Calorim* 57:313–322.
- Al-Saidan SM, Barry BW, Williams AC. 1998. Differential scanning calorimetry of human and animal stratum corneum membranes. *Int J Pharm* 168:17–22.
- Takenouchi M, Suzuki H, Tagami H. 1986. Hydration characteristics of pathologic stratum corneum-evaluation of bound water. *J Invest Dermatol* 87:574–76.
- Middleton JD. 1968. The mechanism of water binding in stratum corneum. *Br J Dermatol* 80:437–450.
- Leveque JL, Escoubez M, Rasseneur L. 1987. Water-keratin interactions in human stratum corneum. *Bioeng Skin* 3:227–242.
- El-Shimi AF, Princen HM. 1978. Water vapor sorption and desorption behavior of some keratins. *Colloid Polym Sci* 256:105–114.
- Spencer TS, Linamen CE, Akers WA, Jones HE. 1975. Temperature dependence of water content of stratum corneum. *Br J Dermatol* 93:159–164.
- Kligman AM, Christophers E. 1963. Preparation of isolated sheets of human stratum corneum. *Arch Dermatol* 88:702–705.
- Weast RC. 1984. Handbook of chemistry and physics, 63rd edition. Boca Raton, FL: CRC press.
- Smith JM, Van Ness HC, Abbott MM. Introduction to chemical engineering thermodynamics, 5th edition. New York: McGraw-Hill Book Co, Inc., pp 668–673.
- Adamson AW. 1976. Physical chemistry of surfaces. New York: John Wiley and Sons, pp 533–538.
- Blank IH. 1952. Factors which influence the water content of the stratum corneum. *J Invest Dermatol* 18:433–440.

33. Bouwstra JA, Gooris GS, Van der Spek JA, Bras W. 1991. Structural investigations of human stratum corneum by small angle X-ray scattering. *J Invest Dermatol* 97:1005–1012.
34. Charalambopoulou GC, Karamertzanis P, Kikkinides ES, Stubos AK, Kanellopoulos NK, Papaioannou AT. 2000. A study on structural and diffusion properties of porcine stratum corneum based on very small angle neutron scattering data. *Pharm Res* 17:1085–1091.
35. Hansen JR, Yellin W. 1972. NMR and infrared spectroscopy studies of stratum corneum hydration. In: Jellinek HHG, editor. *Water structure at the water-polymer interface*. New York: Plenum Press, pp 19–28.
36. Packer KJ, Sellwood TC. 1978. Proton magnetic resonance studies of hydrated stratum corneum. Part 2. Self-diffusion. *Chem Soc J Faraday Trans* 74:1592–1606.
37. Yamamura T, Tezuka T. 1989. The water-holding capacity of stratum corneum measured by $^1\text{H-NMR}$. *J Invest Dermatol* 93:160–164.
38. Kasting GB, Barai ND, Wang T-F, Nitsche JM. 2003. Mobility of water in human stratum corneum. *J Pharm Sci* 92:2326–2340.
39. Cassie ABD. 1945. Absorption of water by wool. *Trans Faraday Soc* 41:458–464.
40. Anderson RL, Cassidy JM, Hansen JR, Yellin W. 1973. Hydration of stratum corneum. *Biopolymers* 12:2789–2802.
41. Anderson RL, Cassidy JM, Hansen JR, Yellin W. 1973. The effect of in vivo occlusion on human stratum corneum hydration-dehydration in vitro. *J Invest Dermatol* 61:375–379.